

A HYBRID FEEDBACK CONTROLLER FOR CAR-LIKE ROBOTS

Combining Reactive Obstacle Avoidance and Global Replanning

Matthias Hentschel, Oliver Wulf, Bernardo Wagner
*Institute for Systems Engineering
University of Hannover
Hannover, Germany*

Keywords: Autonomous mobile robots, motion planning, obstacle avoidance, AGV system.

Abstract: This paper presents a hybrid feedback controller for path control of autonomous mobile robots. The controller combines reactive obstacle avoidance with global path replanning, enabling collision-free navigation along a preplanned path. Avoidance of local obstacles is accomplished by adjusting the vehicle's lateral deviation from the path trajectory reactively. Global path replanning is performed to circumvent obstacles which cannot be avoided locally. In contrast to common approaches, this is done by searching an optimal path returning to the initial trajectory beyond the obstacle. Following the description of the hybrid feedback controller, experimental results will demonstrate the effectiveness of this approach.

1 INTRODUCTION

In the last few years remarkable progress in the localization of autonomous mobile robots has been achieved. Especially the *Monte Carlo Localization* (Daellert et al., 1999) (Wulf et al., 2005) has to be mentioned as a robust and reliable method for global position estimation. The precise localization enables exact navigation of autonomous vehicles along a preplanned trajectory. This is a key requirement for autonomous mobile robots and Automated Guided Vehicle (AGV) systems. This kind of vehicles, e.g. our autonomous robot *RTS-DORA* (see Fig.1) and our *RTS-STILL Robotic Fork Lift* typically serve in industrial environment. In these surroundings robots have to deal with fixed ways and storage places as well as prestructured production processes. By applying the predefined trajectories, a deterministic behaviour of the autonomous robot is achieved. Nevertheless, collision avoidance is a key challenge in these applications, especially if mobile robots and human beings share a common workspace. People and other dynamic obstacles block the robot's path hence making it necessary for the autonomous system to perceive the environment and react dynamically to unforeseen circumstances.



Figure 1: Autonomous mobile robot RTS-DORA.

Principally collision avoidance methods for mobile robots can be divided into global and local approaches. The global techniques, like *road-map*, *cell decomposition* and *potential field* methods (Latombe, 1991) (LaValle, 2006), assume that a complete model of the robot's workspace is available. Generally the global world models are based on sensory input and can be updated by using probabilistic representations (Moravec, 1988). Due to the knowledge about the global obstacle situation, these collision avoidance methods enable global path planning. A complete path from a starting point

to a goal location can be calculated off-line. Unfortunately, these global techniques are not appropriate for fast obstacle avoidance. This is a key feature of local, or reactive obstacle avoidance approaches. These methods typically consider only a small subset of obstacles close to the robot, thus adapting quickly to unforeseen changes in the environment. Well known reactive techniques are *force field methods* (Borenstein and Koren, 1990) and the *dynamic window approach* (Fox et al., 1997). Because of considering only the nearest surrounding close to the robot, local approaches can easily be trapped in local minima such as U-shaped obstacle configurations.

This paper describes a feedback controller that combines both local and global obstacle avoidance techniques. The hybrid controller connects the preferences of both methods thus enabling collision-free navigation along a predefined trajectory. Reactive obstacle avoidance is performed by adjusting vehicle's lateral deviation obstacle-depending to the nominal trajectory. This is fulfilled in real-time by a straightforward algorithm allowing high-speed collision avoidance. To give the local technique the capability of handling path blocking obstacles (like closed doors) and other local minima, global path replanning is performed in cases where obstacles cannot be avoided reactively. Based on an occupancy grid map updated with laser range data, a feasible path is searched by *Dijkstra's algorithm* (Dijkstra, 1959). Similar to the well-known *A* algorithm*, this method represents the global part of the controller. In contrast to common approaches, our algorithm searches an optimal path returning to the initial trajectory behind the obstacle. Based on the search result, the initial trajectory is replanned around the global obstacle. As the recalculation of the complete path is not necessary, this approach is especially effective for long trajectories.

2 HYBRID FEEDBACK CONTROLLER

2.1 Path Tracking

The path which has to be followed by the mobile robot consists of a concatenation of *i* lines and polar splines (Horn, 1997). From a set of predefined waypoints, this trajectory is generated automatically by our motion planner with regards to the kinematic constraints of the vehicle. Additionally for each path

segment a desired speed and driving direction is pre-selectable. With cusps allowed in path trajectory, a robot model similar to Reeds-Shepp's car (Reeds and Shepp, 1990) is assumed. Due to the consideration of robot's nonholonomic constraints in path generation each planned trajectory is driveable in general.

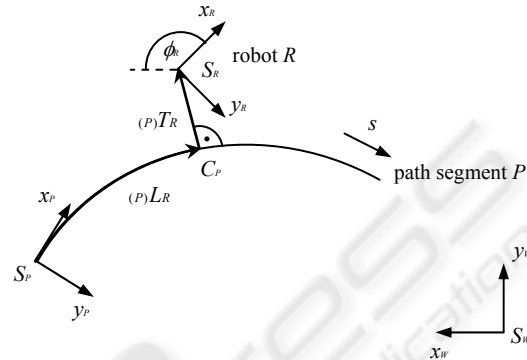


Figure 2: Robot location on a single path segment P.

Trajectory tracking is performed by a cascade controller, combining feedforward and feedback control for high path accuracy. Figure 2 illustrates the significant parameters used in position control. The longitudinal position of the robot *R* on a single path element *P* is denoted as $(P)L_R$ in reference to the local coordinate system S_P of that segment. The transversal displacement $(P)T_R$ is normal to the path *P* (with C_P as the perpendicular foot) and is defined as the distance between the robot position (coordinate system S_R) and the trajectory. The orientation error $(P)\phi_R$ is the difference between the slope of the tangent-line through the point C_P and the robot orientation ϕ_R .

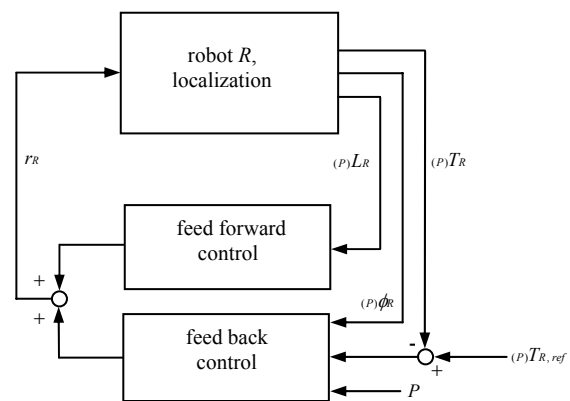


Figure 3: Overview of the closed-loop control system for path tracking.

mobile vehicle in the initial coordinate system S_W , the parameters $(P)L_R$, $(P)T_R$ and $(P)\phi_R$ can be calculated

and used for path control. A fundamental overview of the closed-loop control system is provided by Figure 3. Output of the position controller is defined as r_R , the radius of the curvature which shall be driven by the robot. Within the vehicle's chassis, this set value is transferred into steering commands. The reference input of the position controller is denoted as ${}^{(P)}T_{R,ref}$. For path tracking in the absence of obstacles this parameter will be ${}^{(P)}T_{R,ref}=0$, thus enabling precise piloting of the autonomous robot along the planned path.

2.2 Local Obstacle Avoidance

The reactive obstacle avoidance has to provide a path that circumnavigates obstacles in the local surrounding of the robot. Moreover the transition of narrow corridors and tight doors must be possible even with noisy localization. Koren and Borenstein (1991) discovered that the commonly used *potential field methods (PFM)* often fail between closely spaced obstacles and tend to oscillate in narrow corridors. Above all, PFMs and other reactive techniques like the *dynamic window approach* are designed for guiding a vehicle safely to a single goal location. However, obstacle avoidance along a well-defined trajectory is hard to realize.

In this work we use a straightforward algorithm for reactive obstacle avoidance. This approach adjusts the reference input ${}^{(P)}T_{R,ref}$ (see Fig. 3) of the position controller obstacle-depending, admitting a controllable lateral displacement of the vehicle from the trajectory. With regard to the kinematic constraints of the robot, the deviation of the vehicle is adjusted by the position controller as quickly as possible to ${}^{(P)}T_{R,ref}$.

The lateral displacement ${}^{(P)}T_{R,ref}$ is computed from the sensory input of at least one laser sensor. As we use the planar world assumption, each scan consists of a list of k two-dimensional obstacle points in Cartesian coordinates $D_n=(x_n,y_n)$ with n being the index. All measurements are received in robot coordinates S_R . The first step in assessing ${}^{(P)}T_{R,ref}$ for a single path segment is a transformation of all k measurement points D_n into the coordinate system S_P of the local path element P . The resulting points ${}^{(P)}D_n$ are given by:

$${}^{(P)}D_n = C \cdot D_n + \begin{pmatrix} \cos(\phi_P) & \sin(\phi_P) \\ -\sin(\phi_P) & \cos(\phi_P) \end{pmatrix} (S_R - S_P) \quad (1)$$

with

$$C = \begin{pmatrix} \cos(\phi_P)\cos(\phi_P) + \sin(\phi_P)\sin(\phi_P) & \cos(\phi_P)\sin(\phi_P) - \sin(\phi_P)\cos(\phi_P) \\ \sin(\phi_P)\cos(\phi_P) - \cos(\phi_P)\sin(\phi_P) & \cos(\phi_P)\cos(\phi_P) + \sin(\phi_P)\sin(\phi_P) \end{pmatrix}$$

where ϕ_P is the orientation of the path element's coordinate system S_P in initial coordinates S_W . Next, for each of the l points ${}^{(P)}D_n$ (with $l \subseteq k$), that are normal to the local path element P the longitudinal position ${}^{(P)}L_{D_n}$ as well as the transversal displacement ${}^{(P)}T_{D_n}$ is determined. The result is illustrated by Figure 4.

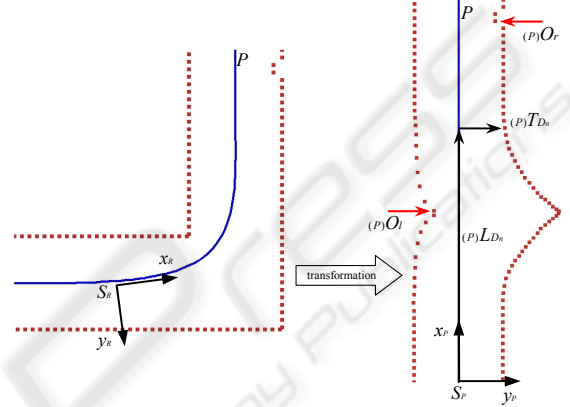


Figure 4: Sensor data (red) in robot coordinates S_R (left) and in transformed coordinates of the local path segment P (right).

The obstacle points which interfere at most with the robot are those closest to the trajectory. With the transformation of the sensor data onto the path, a simple determination of these two points ${}^{(P)}O_l$ and ${}^{(P)}O_r$ (see Fig. 4) is possible. According to the following equation, they are defined by:

$${}^{(P)}O_l = \begin{pmatrix} {}^{(P)}L_{D_n} \\ \max({}^{(P)}T_{D_n}) \end{pmatrix} \quad \begin{aligned} -\infty &\leq {}^{(P)}T_{D_n} < 0, \\ 0 &\leq n < l \end{aligned} \quad (2)$$

$${}^{(P)}O_r = \begin{pmatrix} {}^{(P)}L_{D_n} \\ \min({}^{(P)}T_{D_n}) \end{pmatrix} \quad \begin{aligned} 0 &\leq {}^{(P)}T_{D_n} \leq \infty, \\ 0 &\leq n < l \end{aligned}$$

To interfere with the path tracking of the autonomous robot, at least one of the obstacle points ${}^{(P)}O_l$ and ${}^{(P)}O_r$ must be in the driveway of the vehicle. The width of this area is described by:

$$w = w_R + w_S \quad (3)$$

where w_R is the width of the (symmetric) robot. The parameter w_S specifies the upper bound of an additional safety margin. If sufficient free space is available, this distance is to maintain to obstacles. Unless enough space for w_S is present, e.g. in narrow corridors, the safety margin may be reduced dynamically down to zero.

With the size of the driveway w , the lateral displacement ${}^{(P)}T_{R,ref}$ is finally computed as follows:

$$\begin{aligned} {}^{(P)}T_{R,ref} &= 0 & {}^{(P)}O_{l,T} &\leq -\frac{w}{2}, \\ {}^{(P)}O_{r,T} &\geq \frac{w}{2} & & \end{aligned} \quad (4)$$

$$\begin{aligned} {}^{(P)}T_{R,ref} &= \frac{{}^{(P)}O_{r,T} + {}^{(P)}O_{l,T}}{2} & (5) \\ {}^{(P)}O_{l,T} &> -\frac{w}{2}, \quad {}^{(P)}O_{r,T} &\geq \frac{w_R}{2} \\ {}^{(P)}O_{l,T} &\leq -\frac{w_R}{2}, \quad {}^{(P)}O_{r,T} &< \frac{w}{2} \end{aligned}$$

$$\begin{aligned} {}^{(P)}T_{R,ref} &= {}^{(P)}T_{R,ref} & {}^{(P)}O_{l,T} &> -\frac{w_R}{2}, & (6) \\ {}^{(P)}O_{r,T} &< \frac{w_R}{2} & & \end{aligned}$$

In equation 4, the obstacle points ${}^{(P)}O_l$ and ${}^{(P)}O_r$ are both outside the driveway, hence not interfering with the robot. The reference input ${}^{(P)}T_{R,ref}$ is set to zero. In cases where a single obstacle point is inside the driveway (equation 5), the reference value is defined as the average between ${}^{(P)}O_{l,T}$ and ${}^{(P)}O_{r,T}$. This permits the transition of narrow corridors and tight doors. Additionally, the lateral displacement ${}^{(P)}T_{R,ref}$ is adjusted in dependence of the available free space and limited in its maximum value. Equation 6 defines the limitation of the local obstacle avoidance. In cases both obstacle points are located within an area of the vehicle's width on the trajectory, these (continuous) obstacles are reactively unavoidable.

2.3 Global Path Replanning

The global part of the hybrid feedback controller performs replanning of the original trajectory in case an obstacle situation cannot be avoided locally. As described above, this occurs e.g. if the whole driveway is blocked by an obstacle. In order to replan the original trajectory, an admissible path around the global obstacle is searched. This is achieved by a discrete feasible path planner. For

this, the essential knowledge about the global obstacle situation is represented as a sensory updated occupancy grid map (Moravec, 1988) as shown in Figure 5. With the grid cells of this map a nonempty state space X is defined.



Figure 5: Exemplary occupancy grid map.

For path planning, the initial state $x_I \in X$ is given by the robot's position S_R in front of the global obstacle. From this location the searched path must return to the trajectory behind the obstacle as fast as possible. Differing from common approaches, this requires a set of well-defined goal states $X_G \subseteq X$. Each goal state is part of a section (with the length d) from the original trajectory behind the global obstacle.

With a given x_I and X_G , the searching for the feasible path is performed by *Dijkstra's algorithm* (Dijkstra, 1959). This method discovers the single-source shortest path in a directed graph. The associated costs $l(e)$ for applying each edge e of this graph are deduced from the grid map obstacle-depending (see Fig. 6).

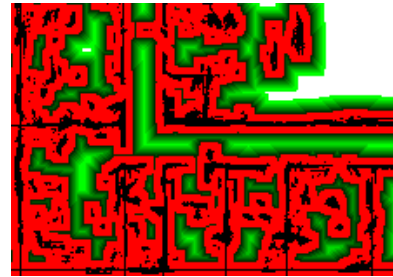


Figure 6: Cost function deduced from the grid map.

Searching for an cost-efficient path is terminated, when a goal state $x_G \in X_G$ is reached by *Dijkstra's algorithm*. The states of the resulting path between x_I and a x_G are denoted as $X_P \subseteq X$. By applying various filter techniques, the number of path states X_P can be reduced to a rudimental set of states $X_W \subseteq X_P$. These states X_W define the vertices of a polygon which represent the optimal path.

With the reduced states X_W , finally replanning of the original trajectory is enabled. Transformed into global waypoints, the set X_W is assigned to our motion planner. Similar to the generation of the original trajectory from a group of given basepoints, the motion planner creates a trajectory with the computed waypoints. Starting from the current robot position, this trajectory permits circumnavigation of the global obstacle and returns to the original planned path behind the obstruction. Here, the newly generated trajectory is concatenated to the original one with a constant transition. As a result, the entire replanned trajectory is available. Due to considering robot's nonholonomic constraints in path generation, this trajectory is driveable in general.



Figure 7: Replanned path (red) returning to the original trajectory (blue, dashed).

By searching a cost-optimal path returning to the original trajectory, only a small fraction of the grid map has to be considered for path replanning (see Fig. 7). As recalculation of the complete path is not required, the computational complexity of this approach remains low.

Finally, a brief overview of the hybrid feedback controller presented in this paper is summarized by Figure 8:

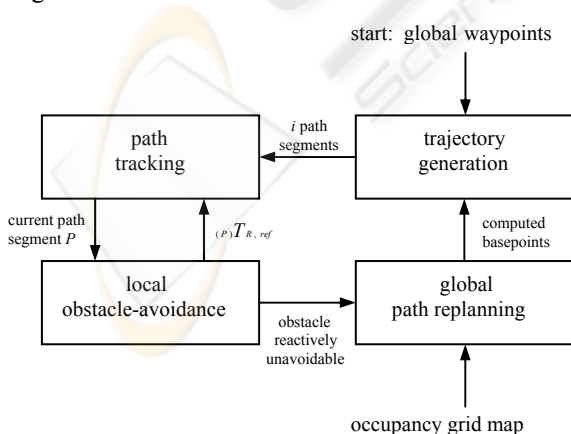


Figure 8: Hybrid feedback controller.

3 EXPERIMENTAL RESULTS

Under real-world condition, the described feedback controller is tested on different robot platform in indoor and outdoor environment.

The experimental results presented here are made exemplary in a real world environment at our institute. With a size of 50m x 20m, the test environment includes doors, narrow corridors and unforeseen obstacles. In this environment the robot is driven fully autonomous along a preplanned path with a maximum speed of 0,8 m/s. For the reactive obstacle avoidance, a maximum lateral displacement of $\pm 0,45$ m is permitted.

The experimental robot consists of an *ActivMedia Pioneer2* based platform (0,5m x 0,5m), equipped with an 2D *Ibeo LD-A* 360° laser range sensor. Data acquisition and all required algorithms for the hybrid feedback controller are computed in real-time on an embedded PC.



Figure 9: Test environment at our institute, lines on the floor mark the preplanned trajectory.

The hybrid feedback controller presented in this paper is used for piloting the robot safely along the preplanned path. Figure 10 shows the results and the obstacle configuration from a top view. The blue line represents the nominal trajectory which is generated by our motion planner from a set of given waypoints. Labelled in red, the real path piloted by the robot is illustrated.

Starting from the point S , the robot firstly encounters a narrow door (Fig. 10a). As soon as the obstacle is recognised, the feedback controller deviates reactively from the original trajectory and passes through the door exactly centred. Subsequent, the robot returns to the original trajectory as soon as it is admitted by the obstacle situation.

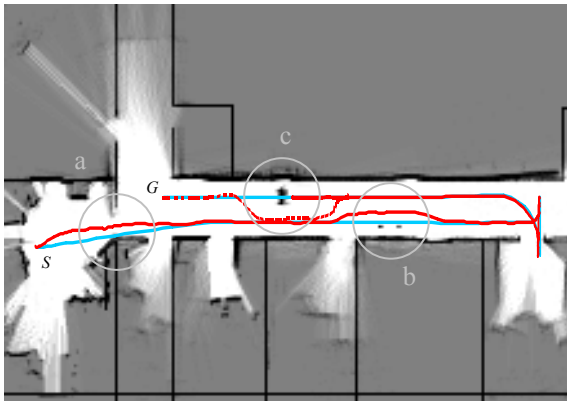


Figure 10: Occupancy grid map of the test environment, including preplanned trajectory (blue) and real path (red).

Next, precise path tracking is performed, until the ladder (Fig. 10b) is identified as an obstacle and avoided locally. In contrast to the previous door transition, sufficient free space is available to maintain the safety margin to the obstacle.

After another door passage while reversing, the mobile robot encounters a global obstacle on its way back (Fig. 9, 10c). This obstacle is reactively unavoidable. In this case, global path replanning is performed by the hybrid feedback controller to circumvent the situation. In Figure 10, the replanned trajectory is illustrated by a dashed line. Using the hybrid feedback controller, this updated trajectory is followed by the robot until the point *G* is reached.

Further evaluation of the hybrid feedback controller has been performed using our mobile robot *RTS-DORA* (see Fig.1). With a total weight of 350 kg and a size of 2,3m x 1,34m the maximal lateral displacement for local avoidance is set to $\pm 1,0$ m. Numerous test runs have been performed on this robot with speeds of up to 2 m/s. These experiments show that our approach can be used for different kinds of vehicles and is not depending on the platform size and speed.

4 CONCLUSION

In this paper we presented a feedback controller for autonomous car-like robots. This controller enables collision-free tracking of a preplanned trajectory. In our approach, the controller combines reactive obstacle avoidance with global path replanning. The experimental results have shown that the

combination of both local and global obstacle avoidance techniques leads to a robust and efficient path controller. Over all, our hybrid feedback controller is capable of piloting safely different mobile robots along preplanned paths in indoor and outdoor environment. With tested speeds up to 2 m/s, the circumnavigation of multiple unexpected obstacles is possible. Next to the prevention of obstacles, our approach enables the transition of narrow corridors and tight doors as well.

REFERENCES

- Borenstein, J. and Koren, Y., 1990, Real-time obstacle avoidance for fast mobile robots in cluttered environments, *ICRA '90, International Conference on Robotics and Automation*.
- Dellaert, F., Fox, D., Burgard, W. and Thrun, S., 1999, Monte carlo localization for mobile robots, *ICRA '99, International Conference on Robotics and Automation*.
- Dijkstra, E.W., 1959, A note on two problems in connexion with graphs, *Numerische Mathematik 1*, pp. 269-271.
- Fox, D., Burgard, W. and Thrun, S., 1997, The dynamic window approach to collision avoidance, *IEEE Robotics and Automation Magazin*.
- Horn, J., 1997, Path control of a mobile robot based on absolute localization by fusion range image and dead-reckoning data, *Fortschrittberichte VDI Reihe 8*, vol 617.
- Latombe, J., 1991, *Robot motion planning*, Kluwer Academic Publishers, Boston.
- LaValle, S.M., 2006, *Planning algorithms*, Cambridge University Press, Cambridge.
- Moravec, H.P., 1988, Sensor fusion in certainty grids for mobile robots, *AI Magazine*, vol 9, summer 1988, pp. 61-74.
- Reeds, J.A. and Shepp, L.A., 1990, Optimal paths for a car that goes both forwards and backwards, *Pacific Journal of Mathematics*, 145(2): 367-393
- Koren, Y. and Borenstein, J., 1991, Potential field methods and their inherent limitations for mobile robot navigation, *ICRA '91, International Conference on Robotics and Automation*.
- Wulf, O., Khallaf-Allah, M. and Wagner, B., 2005. Using 3D data for monte carlo localization in complex indoor environments, *ECMR '05, European Conference on Mobile Robots*.